

Keywords: transport speed; vibrations; vibratory conveyor; dynamic eliminator; transport stopping; feeder

Piotr CZUBAK^{1*}, Witold SURÓWKA²

TRANSPORT FEATURES OF A NEW, SELF-ATTUNED CONVEYOR

Summary. The new vibratory conveyor destined for the accurate dosing of materials was investigated in the present work. The possibilities of the system to transport materials in the circum-resonant zone were tested analytically, as well as by simulations. The optimal work point of the system, which allowed a decrease in the amplitude of eliminator vibrations on its suspension due to operations on the resonance slope, was determined. Transport velocities depending on the excitation frequency and feed mass were determined by simulations. The results were verified on the conveyor of industrial dimensions designed and built in accordance with the patent application.

1. INTRODUCTION

The transport abilities of the new vibratory conveyor (patented by the authors) operating in the resonance zone were investigated in this study. The conveyor is used for transporting and dosing loose materials or objects with small dimensions, providing the possibility of maintaining a constant transport velocity regardless of the feed mass and in spite of the application of a small and relatively cheap electro-vibratory drive. This is a unique property of the inertial drive that does not change its characteristics during operation [1]. This conveyor also provides the possibility of the precise dosage of materials, as described in previous papers [2]

Very often, in the production line, the essential property of the vibratory conveyor is the possibility of maintaining a constant transport velocity regardless of the feed mass when a small energy-saving drive is applied [3]. To the authors' knowledge, conveyors of inertial drive providing such a possibility do not exist.

Classic conveyors with inertial drives involve a decrease in the coefficient of throw according to Equation (1), which translates to a decrease in transport velocity at higher masses of feed [4].

$$k_t = \frac{m_v e \omega^2 \sin \beta}{(m_t + m_v + m \sin^2 \beta) \cdot g} \quad (1)$$

where:

e – radius of gyration,
 β – angle of direction of motion,
 m_v – rotating mass,
 m_t – trough mass,
 m – mass of the feed.

In our case, an increase in the feed mass causes a decrease in the coefficient of throw. However, the resonance frequency of the second resonance is simultaneously shifted, which moves the system nearer to the resonance peak, which, in turn, maintains the vibration amplitude at the same frequency.

¹ AGH University of Science and Technology; Mickiewiczza av. 30, 30-059 Kraków, Poland; e-mail: czubak@agh.edu.pl; orcid.org/0000-0001-8030-7173

² AGH University of Science and Technology; Mickiewiczza av. 30, 30-059 Kraków, Poland; e-mail: witold@agh.edu.pl; orcid.org/0000-0002-1288-7759

* Corresponding author. E-mail: czubak@agh.edu.pl

Such behavior guarantees the constant transport velocity of various feed masses, and this is a unique property of vibratory conveyors.

The only way to maintain the constant velocity of the classic conveyor is to apply a drive of the kinematic excitation. This solution has several faults, of which the main ones are movable joints, which do not warrant durability under industrial conditions. In addition, such a solution transfers significant forces to foundations.

2. STRUCTURE OF THE ANALISED CONVEYOR

The new patented vibratory conveyor [1] is presented in Fig. 1. This conveyor is built of a classic trough (1) of mass m_r and moment of inertia J_r , is elastically supported (2) with a stiffness of $k_{x,y}$ and damping of $b_{x,y}$, and is distanced from the center of mass by $l_{1,2}$ on a stiff base in a horizontal position. It is also equipped with a system of two counter running vibrators (3) of masses $m_{1,2}$, moments of inertia $J_{1,2}$, and radiuses of gyration $e_{1,2}$, which are suspended to the trough at angle β and distanced from the mass center by $a_{1,2}$ and $h_{1,2}$. They are powered with electric torque $M_{el1,2}$ described in Equation (11). In the steady state, vibrators are synchronized and counter running, providing the resultant rectilinear force, which passes through the mass center of the trough system, as well as through the center of its suspension system.

The additional mass (4)—with a value of m_e and a moment of inertia J_e , on its own suspension (5) of a stiffness of k_τ and damping of b_τ —is added to the main mass (1) and has its own additional degree of freedom ‘ τ .’ In general, the main masses move together on x, y following the rotation direction α ; the only exception is ‘ τ ’ for the eliminator (4).

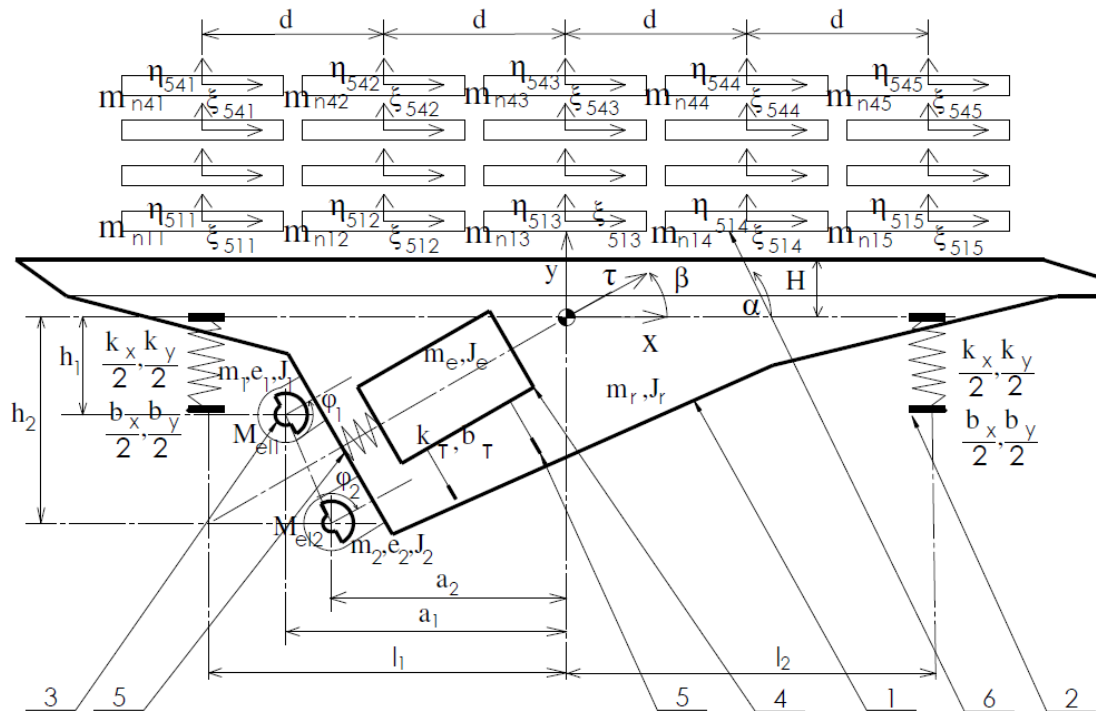


Fig. 1. Schematic representation of the conveyor (according to the invention)

The aim of this additional mass is to eliminate the trough vibrations at a proper control of the vibrator's excitation frequency in accordance with Frahm's eliminator principle [5, 6] when the excitation frequency is calculated as follows:

$$\omega = \sqrt{k_\tau / m_e} \quad (2)$$

Trough vibration stoppage causes feed transport stoppage (6) [2]. Feed is digitized to particles of masses m_{n11} to m_{n45} , which can move freely in two directions: η and ξ . The whole feed rests on the trough, the surface of which is distanced from the mass center by ‘H.’ Moreover, every column of the feed particles is distanced from each other by ‘d.’ As for the vertical position, particles rest on each other and the trough. It was pointed out in this study that when the conveyor is operating within the circum-resonant zone of the second resonance, it is possible to obtain the constant transport velocity regardless of the conveyor load. In addition, the conveyor in this zone acts as the resonance vibro-insulated conveyor. It occurs in such a way due to the additional mass, which provides the device with the proper characteristics through the additional resonance.

Classic resonance conveyors operate on the trough mass resonance, which, in practice, causes significant forces to be transferred to the foundations due to the high stiffness of the conveyors’ suspension. A fault of such conveyors also constitutes a significant influence of the conveyor mass on its transport velocity due to resonance damping (among other reasons) [7].

The analyzed conveyor does not have the abovementioned faults. Its resonance at the working frequency is related to the suspension stiffness of the additional mass, which is not connected to foundations. The main suspension is relatively soft, and therefore, it does not transfer significant forces to the foundations at the work amplitude.

The constant transport velocity is achieved without the need to control the conveyor’s rotational speed. This is due to the fact that the trough mass also has only a small influence on the second resonance frequency, on which the growing slope of the conveyor operates. An increase in the trough mass shifts the second resonance frequency towards lower frequencies. Since the feed mass influences the trough mass [4,8], the increase in the feed mass causes the resonance frequency to shift spontaneously. In accordance with the analyses performed in these studies, at the angle trough vibration of 30° inclination to the horizontal line, $\frac{1}{4}$ of the feed mass should be added. Of course, this significantly influences the shifting of the first resonance [9] and—albeit to a much smaller degree—the second resonance.

Theoretically, instead of the first resonance, there should be three resonances. However, when stiffnesses k_x and k_y are the same and the excitation force passes through the center of the machine’s mass, these three resonances merge into one.

The frequency of the second resonance is mainly related to the mass and stiffness of the eliminator suspension. This is why, at a constant frequency, the feed decreases the resonance amplitude on the one hand and causes the device to operate near the top of the resonance amplitude on the other hand. In fact, despite the application of a very small inertial drive, the constant transport velocity is obtained regardless of the feed mass; however, the resonance frequency remains below the excitation frequency only until the moment when the feed ‘will shift.’

3. SIMULATION INVESTIGATIONS

In order to determine the transport velocity in dependence on the system excitation frequency, the system presented in Fig. 1 (loaded with the feed) was investigated. The mathematical model of such a system essentially contains six equations, one for each degree of freedom. Additionally, there are 20 feed particles that can move in two independent directions, yielding another 40 equations.

The presented mathematical model calculated from Lagrange’s equations of the second kind contains Matrix Equation (3) (describing the machine movement), Equation (11) (describing the electromagnetic moment of drive motors), Equations (9) and (10) (determining the movements of successive feed layers), and Equations (7) and (8) (describing normal and tangent interactions in between feed layers, as well as between the feed layer and machine body) [10-12].

$$[M] \cdot [\ddot{q}] = [Q] \quad (3)$$

$$M = \begin{bmatrix} m_r + m_1 + & 0 & m_1 h_1 + m_2 h_2 & m_1 e_1 \sin(\varphi_1) & m_2 e_2 \cos(\varphi_2) & m_e \cos \beta \\ m_2 + m_e & m_r + m_1 + & -m_1 a_1 - m_2 a_2 & m_1 e_1 \cos(\varphi_1) & m_2 e_2 \sin(\varphi_2) & m_e \sin \beta \\ 0 & m_2 + m_e & & & & \\ m_1 h_1 + m_2 h_2 & -m_1 a_1 - m_2 a_2 & m_2(h_2^2 + a_2^2) + m_1(h_1^2 + a_1^2) & m_1 h_1 e_1 \sin(\varphi_1) - & m_2 h_2 e_2 \cos(\varphi_2) - & 0) \\ & + J_r + J_e & & m_1 a_1 e_1 \cos(\varphi_1) & m_2 a_2 e_2 \sin(\varphi_2) & \\ m_1 e_1 \sin(\varphi_1) & m_1 e_1 \cos(\varphi_1) & m_1 h_1 e_1 \sin(\varphi_1) - & m_1 e_1^2 + J_{01} & 0 & 0 \\ & & m_1 a_1 e_1 \cos(\varphi_1) & & & \\ m_2 e_2 \cos(\varphi_2) & m_2 e_2 \sin(\varphi_2) & m_2 h_2 e_2 \cos(\varphi_2) - & 0 & m_2 e_2^2 + J_{02} & 0 \\ & & m_2 a_2 e_2 \sin(\varphi_2) & & & \\ m_e \cos \beta & m_e \sin \beta & 0 & 0 & 0 & m_w \end{bmatrix} \quad (4)$$

$$\ddot{q} = [\ddot{x} \quad \ddot{y} \quad \ddot{\alpha} \quad \ddot{\varphi}_1 \quad \ddot{\varphi}_2 \quad \ddot{\tau}]^T \quad (5)$$

$$Q = \begin{bmatrix} m_2 e_2 \dot{\varphi}_2^2 \sin(\varphi_2) - m_1 e_1 \dot{\varphi}_1^2 \cos(\varphi_1) - 2k_x(x + h\alpha) - 2b_x(\dot{x} + h\dot{\alpha}) - T_{1(01)} - T_{1(02)} - T_{1(03)} - T_{1(04)} - T_{1(05)} \\ -m_2 e_2 \dot{\varphi}_2^2 \cos(\varphi_2) + m_1 e_1 \dot{\varphi}_1^2 \sin(\varphi_1) - k_y(y + l_1 \alpha) - k_y(y - l_2 \alpha) - b_y(\dot{y} + l_1 \dot{\alpha}) - b_y(\dot{y} - l_2 \dot{\alpha}) - F_{1(01)} - F_{1(02)} - F_{1(03)} - F_{1(04)} - F_{1(05)} \\ -m_1 h_1 e_1 \dot{\varphi}_1^2 \cos(\varphi_1) - m_1 a_1 e_1 \dot{\varphi}_1^2 \sin(\varphi_1) + m_2 h_2 e_2 \dot{\varphi}_2^2 \sin(\varphi_2) + m_2 a_2 e_2 \dot{\varphi}_2^2 \cos(\varphi_2) - 2k_x h^2 \alpha - 2k_x h \dot{x} - 2b_x h \dot{x} - 2b_x h^2 \dot{\alpha} - k_y(y + l_1 \alpha) l_1 + \\ k_y(y - l_2 \alpha) l_2 - b_y(\dot{y} + l_1 \dot{\alpha}) l_1 + b_y(\dot{y} - l_2 \dot{\alpha}) l_2 (T_{1(01)} + T_{1(02)} + T_{1(03)} + T_{1(04)} + T_{1(05)}) H_r + 2dF_{1(01)} + dF_{1(02)} - dF_{1(04)} - 2dF_{1(05)} \\ \mathcal{M}_{el1} - b_{s1} \dot{\varphi}_1^2 \operatorname{sgn}(\dot{\varphi}_1) - m_1 g e_1 \cos(\varphi_1) \\ \mathcal{M}_{el2} - b_{s2} \dot{\varphi}_2^2 \operatorname{sgn}(\dot{\varphi}_2) - m_2 g e_2 \cos(\varphi_2) \\ -k_\tau \tau - b_\tau \dot{\tau} \end{bmatrix} \quad (6)$$

where:

$F_{j,(j-1,k)}$ – normal component of j -layer pressure on $j-1$ in k -column,

$T_{j,(j-1,k)}$ – tangent component of j -layer pressure on $j-1$ in k -column,

j – indicator of the material layer, $j=0$ is related to the machine body,

k – indicator of the material layer column.

When contact between layers occurs, forces are applied in the normal $F_{j,(j-1,k)}$ and tangent $T_{j,(j-1,k)}$ components. Meanwhile, when there is a lack of contact, the forces are equal to zero:

$$F_{j,(j-1,k)} = (\eta_{j-1,k} - \eta_{j,k})^p \cdot k \cdot \left\{ 1 - \frac{1-R^2}{2} \left[1 - \operatorname{sgn}(\eta_{j-1,k} - \eta_{j,k}) \cdot \operatorname{sgn}(\dot{\eta}_{j-1,k} - \dot{\eta}_{j,k}) \right] \right\} \quad (7)$$

The force in the tangent direction originating from friction is calculated as follows:

$$T_{j,(j-1,k)} = -\mu F_{j,(j-1,k)} \operatorname{sgn}(\dot{\xi}_{j,k} - \dot{\xi}_{j-1,k}) \quad (8)$$

Equations of motion in directions ξ and η of individual feed layers (while taking into account the conveyor influence on lower feed layers), are of the following form:

$$m_{nj,k} \ddot{\xi} = T_{j,(j-1,k)} - T_{j+1,(j,k)} \quad (9)$$

$$m_{nj,k} \ddot{\eta} = -m_{nj,k} g + F_{j,(j-1,k)} - F_{j+1,(j,k)} \quad (10)$$

$$\mathcal{M}_{eli} = \frac{2M_{ut}(\omega_{ss} - \dot{\varphi}_i) \cdot (\omega_{ss} - \omega_{ut})}{(\omega_{ss} - \omega_{ut})^2 + (\omega_{ss} - \dot{\varphi}_i)^2} \quad (11)$$

where:

M_{el} – moment generated by drive motors,

M_{ut} – break-down torque of drive motors,

ω_{ss} – synchronous frequency of drive motors,

ω_{ut} – stall frequency of drive motors.

Such a non-linear mathematical model could be solved with numerical analysis. Runge-Kutta's algorithm was chosen to solve this system of equations. The time step of the simulation was $1 \cdot 10^{-5}$ s, which is sufficiently dense to obtain proper results of feed and trough contact phenomena. The numerical model was calculated in the Pascal environment, and the set of constants used is listed in Table 1 below.

Table 1

Parameters used to perform the simulation

Definition	Unit	Symbol	Value
linear dimension	<i>m</i>	l_1	0.177
linear dimension	<i>m</i>	l_2	0.177
linear dimension	<i>m</i>	h	0
linear dimension	<i>m</i>	h_1	0.045
linear dimension	<i>m</i>	h_2	0.177
linear dimension	<i>m</i>	a_1	0.231
linear dimension	<i>m</i>	a_2	0.155
linear dimension	<i>m</i>	d	0.35
linear dimension	<i>m</i>	H	0.12
radius of a vibrator unbalance	<i>m</i>	e_1	0.02
radius of a vibrator unbalance	<i>m</i>	e_2	0.02
total stiffness of suspension for eliminator's suspension	<i>N/m</i>	k_τ	320 002
stiffness of suspension	<i>N/m</i>	k_x	71 040
stiffness of suspension	<i>N/m</i>	k_y	71 040
coefficient of viscous damping	<i>Ns/m</i>	b_x	1582 / φ_1
coefficient of viscous damping	<i>Ns/m</i>	b_y	1582 / φ_1
total coefficient of viscous damping for eliminator's suspension	<i>Ns/m</i>	b_τ	298 / φ_1
mass of the trough	<i>kg</i>	m_r	28
rotating mass I	<i>kg</i>	m_1	0.0415 or 0.083
rotating mass II	<i>kg</i>	m_2	0.0415 or 0.083
mass of the eliminator	<i>kg</i>	m_e	26
central moment of inertia of the excitation I	<i>kgm²</i>	J_1	0.001
central moment of inertia of the excitation II	<i>kgm²</i>	J_2	0.001
central moment of inertia of the trough	<i>kgm²</i>	J_r	2.56
central moment of inertia of the eliminator	<i>kgm²</i>	J_e	0.9
break-down torque	<i>Nm</i>	M_{ut}	5
synchronous speed	<i>rad/s</i>	ω_{ss}	Variable
break-down torque speed	<i>rad/s</i>	ω_{ut}	Variable
restitution coefficient	-	R	0.13
coefficient of friction	-	μ	0.4
Hertz-Staierman stiffness	<i>N/m</i>	k_s	10 ⁸
Hertz-Staierman constant	-	p	1
coefficient of viscous damping in bearing	<i>Nms</i>	b_{s1}	0.0009
coefficient of viscous damping in bearing	<i>Nms</i>	b_{s2}	0.0009

The simulation model assumes that the virtual trough is of an infinite length and that the particles are constantly moving along its length. However, this model does not assume that the particles change their velocity from zero to the nominal one when falling on the trough.

Investigations indicate that the influence of this change on the system is minimal and is related only to the momentum change at the moment when the particle contacts the trough. This, in practice, converts into a constant pressing force in a horizontal direction. The force value for this conveyor does not exceed 1.5 [N], and it only stretches transverse the springs of the main suspension. In reality, particles falling on the trough almost immediately obtain the nominal velocity, which is constant along the entire length of the trough. In industrial practice (and in our simulations), the height of its bed is constant at the whole length of the trough at a constant speed of supplying feed (but not in amounts higher than the conveyor output).

In some cases, the simulation of the bed height is not determined, but it is regulated by means of the feed mass. We consider velocity as the average velocity of all particles and propose that it properly presents the bed movement. This was confirmed by the laboratory tests. An example of the waveform of the trough vibration and feed layers moving on this trough is given in Fig. 2.

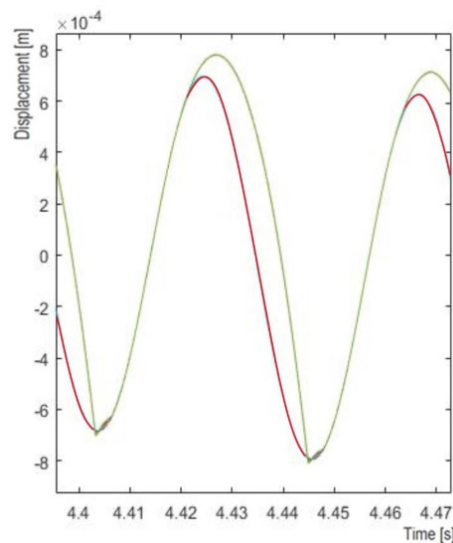


Fig. 2. Exemplary feed movement (green line) on the through surface (red line)

There is a possibility of fluidizing the very fine (small elements) feed, which, in practice, delays the process of falling on the trough but does not cause any lack of momentary contacts, as described in the simulation model by the contact force equation. This force occurs at the moment of hitting the trough and influences the machine's operation. Therefore, not only does the trough movement influence the feed, but feedback coupling also occurs. The feed is not treated as one element in the simulation model. During the contact, successive elements hit the trough in a very short time. Damping in the feed occurs since the contact force equation contains the coefficient of restitution, and consequently, the additional damping (which is dependent on the feed mass) is introduced into the system. This additional damping is treated as dry friction.

4. RESULTS OF SIMULATION INVESTIGATIONS

Data series, which are solutions to equations of motions in time, constitute the simulation results. This means that we obtained displacements, velocities and accelerations for all 46 degrees of freedom. Since the presentation of all results would cause a significant increase in this paper's length, the authors decided to focus on transport velocity only. This velocity was determined every time by averaging the velocities of all 20 feed particles. The data representing various feed masses and two values of the inertial excitation force are presented in Figs. 3-5. The rotational speed of synchronized vibrators was determined directly from simulations.

The transport velocity is maintained, regardless of the feed mass, by the self-control of the conveyor. This phenomenon can be explained as follows. A feed influences a conveyor in two ways: it

damps the trough movement, thereby lowering the amplitude, and it influences the second resonance by shifting it as if to add $\frac{1}{4}$ of the feed mass to the resonating mass [4].

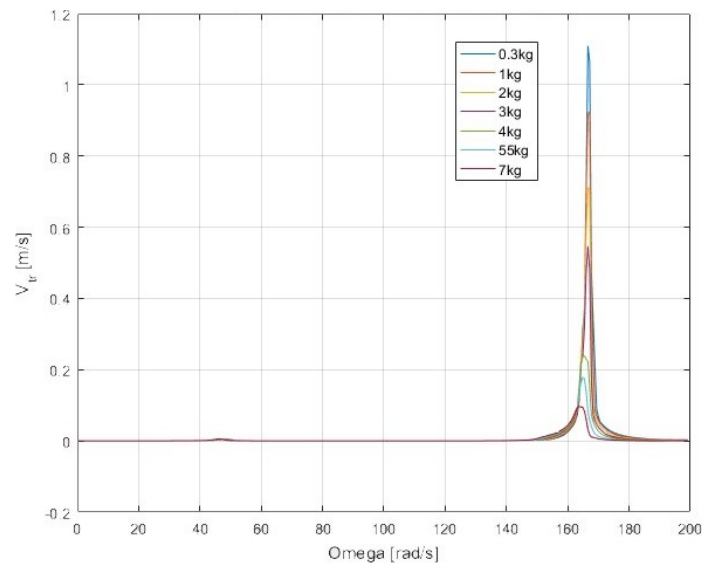


Fig. 3. Average transport velocity of the feed series on the conveyor at the nominal excitation of 40 N

Thus, on the one hand, together with a higher feed mass, the amplitude decreases by a higher feed load, while, on the other hand, the resonance is shifted nearer to the work point, which increases the amplitude in such a way that it ultimately remains unchanged despite the feed addition. Considering that the operation occurs at the same frequency, the constant transport velocity is obtained regardless of the feed mass. This was confirmed by the simulation and experimental tests performed during this study.

The series of amplitude-frequency characteristics of the performing element at the harmonic excitation amplitude of 40 N for various feed masses are presented in Figs. 3 and 4. As seen in the diagram, the transport velocity of $V_{tr}=0.35$ [m/s] is obtained at a constant frequency of 166 rad/s regardless of the feed mass, up to a mass exceeding 2 kg.

The system operates in such a way that, at a small mass of the feed, the resonance and, consequently, the maximum velocity occurs at 167 rad/s. Thus, when the frequency is set to 166 rad/s, we operate on the resonance slope; meanwhile, when the feed mass equals 4 kg, the resonance occurs at 163 rad/s, which means that we operate exactly in the resonance. The result of such behavior of the device is a constant transport velocity regardless of the feed load since the system is self-attuned.

Of course, the amplitude-frequency characteristic is consistent with the transport velocity. However, it should be kept in mind that the coefficient of throw increases with the frequency square, and therefore, feed movement does not occur at the first resonance. It should also be mentioned that the real geometrical limitations of the eliminator allow an amplitude of only 12 mm to be achieved, which reduces the resonance characteristic of lighter feeds [13]. The real system stops behaving like the system with an eliminator, and amplitudes do not increase, which is favorable considering the structure's safety.

The diagrams show that, at the excitation amplitude of 40 [N], it is possible to obtain the constant transport velocity of 0.35 [m/s] for the feed mass of 3 kg, while at the excitation of 80 [N], the same velocity can be obtained for the feed mass of app. 5 kg (Fig. 5). It should be emphasized that such small excitations are sufficient since this conveyor operates in the resonance zone, not the typical resonance conveyor where the main suspension, being of high stiffness, causes the transferring of significant forces to the foundation.

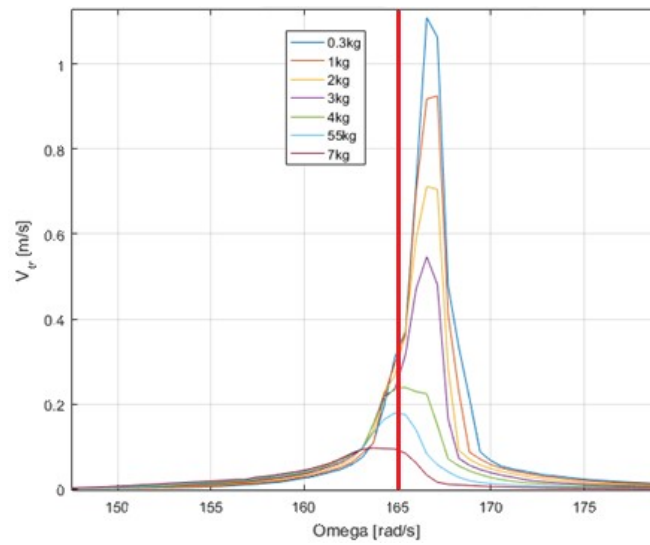


Fig. 4. Magnification of the resonance zone from Fig. 3

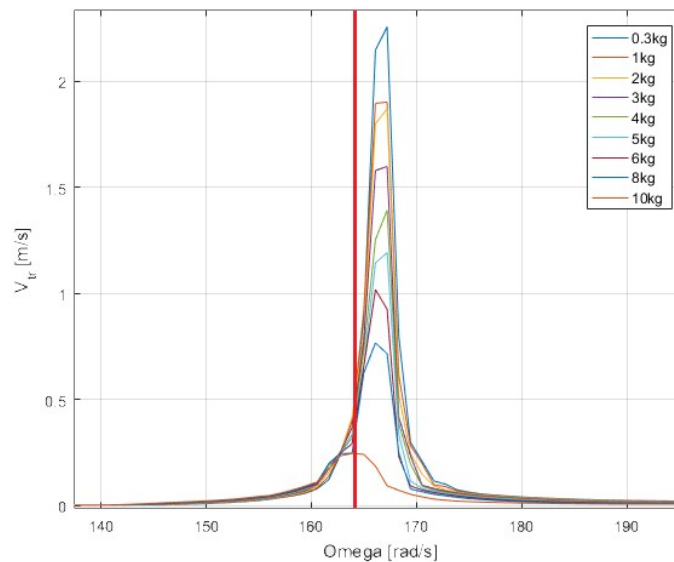


Fig. 5. Average transport velocity of the feed series on the conveyor at the nominal excitation of 80 N

5. TESTING THE CONVEYOR ON THE INDUSTRIAL SET-UP

The successive stage of controlling the simulation correctness constituted the analysis of the trough motion in the work direction by means of the speed camera of the GOM Metrology system, allowing movements of special markers placed on the trough to be traced (Fig. 6). From the figure, one can see that the markers follow the same direction as the same amplitudes. This guarantees that the main mass is in linear motion, which also means that the self-synchronization of the two vibrators is correct and that we can expect steady transportation velocity along the trough. These accurate tests allowed us to draw the quasi-stable characteristic amplitude of the trough from the work point, thereby slowly and uniformly reducing the excitation frequency up to the stoppage.

Tests were performed with the sampling frequency of 100Hz, which satisfies the Whittaker-Nyquist-Shannon-Kotelnikov sampling theorem, up to 50Hz of the excitation frequency. Such seldom sampling, which was limited by the equipment, makes it necessary to use a larger data series to find

representative results. This means that, in practice, slow changes are necessary in the excitation frequency during a measurement.

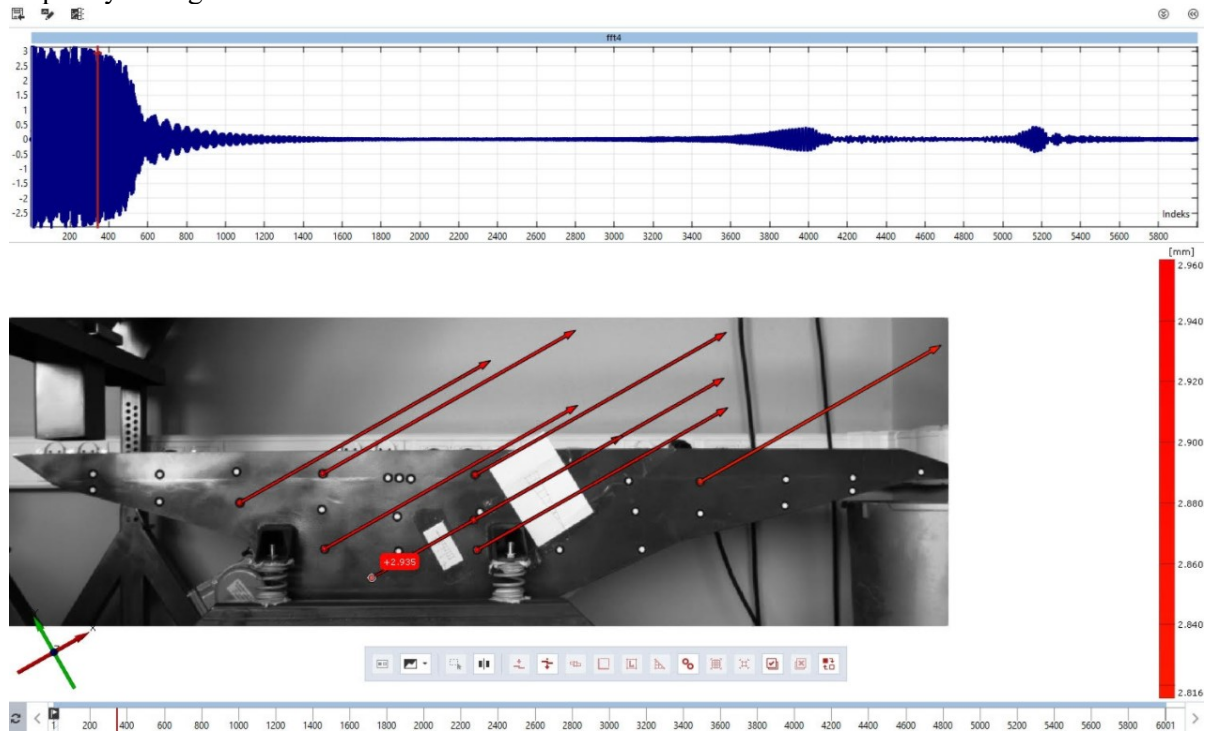


Fig. 6. Screen capture of GOM software used while studying the machine’s movement, oscillating in its work direction, recorded with a high-speed camera

In diagrams from the real measurements (Fig. 6), four resonance amplitudes are seen: three of the device passing through resonances related to the main suspension and one (the main resonance) related to the additional mass of the eliminator. In the simulation results (mentioned previously), only one resonance was visible.

The first three resonances resulted from a slightly different elasticity of real springs in the x and y directions and inaccurate excitation passage through the machine’s center of gravity. However, they have no influence on the conveyor operation in the vicinity of the main resonance related to the mass of the eliminator.

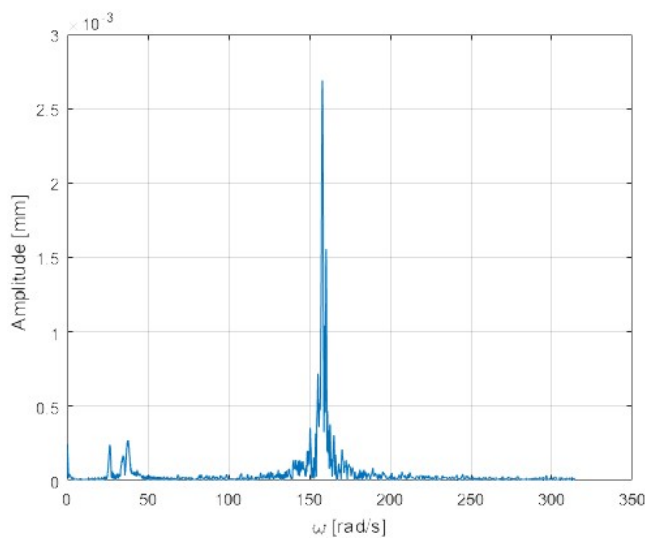


Fig. 7. Spectrum analysis of the course from Fig. 6

Fig. 8 presents the comparison of amplitudes obtained during simulations with real amplitudes of the conveyor at a negligible load of a feed. The blue line represents the characteristic determined from the displacement notation (Fig. 6) by means of Fast Fourier Transform (FFT), shown in Fig. 7. The high compatibility of the results, especially in the zone of the target resonance, is depicted in the diagram. In consideration of structural reasons, the investigations of the real conveyor were performed for a trough amplitude equal to 3 mm, which is the maximum available amplitude for this structure.

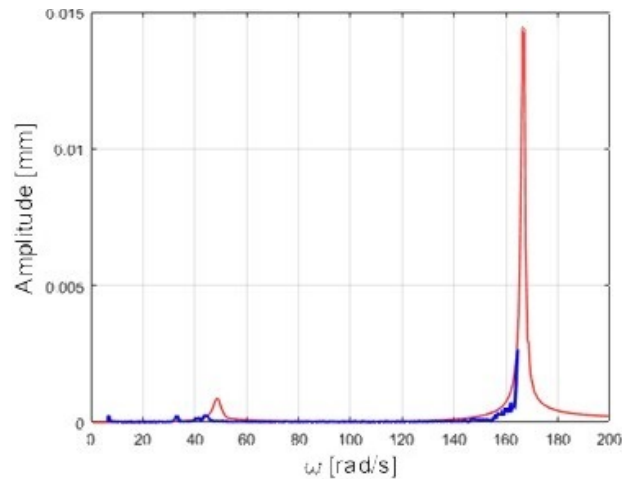


Fig. 8. Frequency analysis of the measurement of the quasi-stable empty conveyor, excited by a force of 80 N, overlapped on the frequency characteristic of the conveyor, obtained from simulations at a negligible feed load (0.3 kg)

5.1. Investigations in the Work Point Under the Feed Load

The transport velocity determination for various feed masses, as the excitation frequency function, is very difficult in the laboratory research set-up. It is difficult due to the necessity of maintaining and controlling the feed mass on the operating conveyor. Thus, the authors focused on showing the dependence of the transport velocity on the feed mass at a constant excitation frequency, which we determined as the nominal velocity (165 rad/s).

Several feed loading tests at frequencies corresponding to nominal transport parameters (165 rad/s) were performed in order to verify whether the conveyor will operate under industrial conditions according to the expectations and will transport the feed with a constant velocity regardless of its mass. The accurate speed of vibrators was controlled by means of the stroboscopic lamp. It should be mentioned that the rotational speed was very stable because we investigated the system for a 10% unbalanced nominal electrovibrator, which means that motors were significantly over-motored for such a system, which caused their operation to remain highly stable. This was the case for both the 40- and 80-N harmonic force excitations (Fig. 9).

Tests on the laboratory research set-up confirmed the results obtained from numerical simulations. Differences in values between simulations and measurements reached a maximum of 10%. This is a highly satisfactory result, especially when the machine operation in the resonance zone is taken into account.

6. CONCLUSIONS

- To the authors' knowledge, the conveyor of a new structure presented in this work is the only double inertial drive conveyor that allows feed transport with a constant velocity without additional controlling regardless of the mass of the feed.

- Investigations performed in this study indicate the possibility of material transport by a conveyor equipped with a small excitation module; however, its unchanging characteristic can be obtained only for a limited loading.
- When a higher drive is applied, the conveyor can transport larger masses of the feed with a constant velocity.
- The limitation of the eliminator amplitude protects the conveyor against breaking down.
- The conveyor structure also allows a very precise dosage of the feed (revealed already in a previous paper [2]).

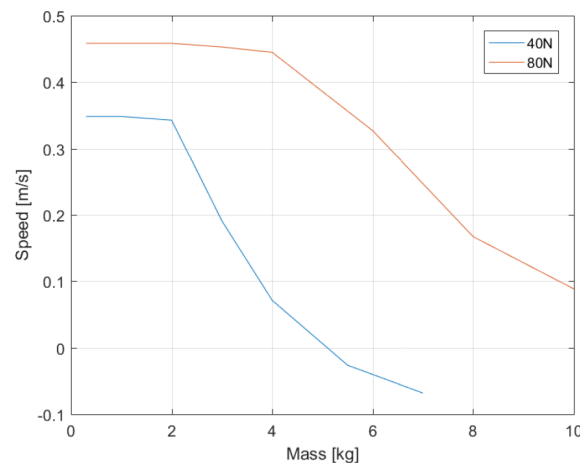


Fig. 9. Survey of the transportation velocities of conveyors excited with 40-N and 80-N forces versus a series of loads with 165 rad/s speed

Acknowledgments

The work is included in the framework of the Department of Mechanics and Vibroacoustics. 16.16.130.942

References

1. PL 239290 A1. Vibratory Conveyor. PL. (Surówka, W. & Czubak, P.) Publ. 6.08.2021.
2. Czubak, P. & Surówka, W. Influence of the excitation frequency on operations of the vibratory conveyor allowing for a sudden stopping of the transport. *Vibrations in Physical Systems*. 2020. P. 1-12.
3. Despotovic, Ž.V. & Ribić, A.I. & Terzić, M.V. A Comparison of Energy Efficiency of SCR Phase Control and Switch Mode Regulated Vibratory Conveying Drives. *IX Symposium Industrial Electronics INDEL 2012*. Banja Luka, November 01-03, 2012. P. 103-110.
4. Michalczyk, J. & Cieplak, G. Selection of the vibrator in the vibration machine taking into consideration the disturbances generated by collisions with feed. *Mechanika*. 2000. Vol. 19. No. 2. P. 221-232.
5. US 989958 A. Device for Damping Vibrations of Bodies. US. (Frahm, H.) Publ. 18.04.1909.
6. Shen, Y. & Xing, Z.B. & Yang, S. & Sun, J. Parameters optimization for a novel dynamic vibration absorber. *Mechanical Systems and Signal Processing*. 2019. Vol. 133. No. 106282.
7. Despotovic, Ž.V. & Urukalo, D. & Lečić, M.R. & et al. Mathematical modeling of resonant linear vibratory conveyor with electromagnetic excitation: simulations and experimental results. *Applied Mathematical Modelling*. 2017. Vol. 41. P. 1-24.
8. Czubak, P. Reduction of forces transmitted to the foundation by the conveyor or feeder operating on the basis of the Frahm's eliminator, at a significant loading with feed. *Archives of Mining Sciences*. 2012. Vol. 57. No. 4. P. 1121-1136.

9. Ganapathy, S. & Parameswaran, M.A. Effect of material loading on the starting and transition over resonance of a vibratory conveyor. *Mechanism and Machine Theory*. 1987. Vol. 22. No. 2. P. 169-176.
10. Bednarski, Ł. & Michalczyk, J. Modelling of the Working Process of Vibratory Conveyors Applied in the Metallurgical Industry. *Archives of Metallurgy and Materials*. 2017. Vol. 62. No. 2. P. 721-728.
11. Michalczyk, J. Phenomenon of force impulse restitution in collision modelling. *Journal of Theoretical and Applied Mechanics*. 2008. Vol. 46. No. 4. P. 897-908.
12. Jiao, C. & Liu, J. & Wang, Q. Dynamic Analysis of Nonlinear Anti-Resonance Vibration Machine Based on General Finite Element Method. *Advanced Materials Research*. 2012. Vol. 443-444. P. 694-699.
13. Sokolov, I.J. & Babitsky, V.I. & Halliwell, N.A. Autoresonant vibro-impact system with electromagnetic excitation. *Journal of Sound and Vibration*. 2007. Vol. 308. Nos. 3-5. P. 375-391.

Received 08.08.2021; accepted in revised form 14.09.2022